ELSEVIER

Measurements of ultrafine particle concentrations and size distribution in an iron foundry

Yu-Hsiang Cheng [a],*, Yen-Chi Chao [a], Cheng-Han Wu [b], Chuen-Jinn Tsai [b], Shi-Nian Uang [c], Tung-Sheng Shih [c]

[a] *Department of Safety, Health and Environmental Engineering, Mingchi University of Technology, 84 Gungjuan Road, Taishan, Taipei 24301, Taiwan*
[b] *Institute of Environmental Engineering, National Chiao Tung University, 75 Poai St., Hsinchu City 30068, Taiwan*
[c] *Institute of Occupational Safety and Health, Council of Labor Affairs, Executive Yuan, 99, Lane 407, Hengke Road, Shijr, Taipei 22143, Taiwan*

Abstract

The number and surface area concentration of ultrafine particles in an iron foundry is of interest as freshly generated ultrafine particles are produced by metal melting, pouring and molding processes. This study measured the number and surface area concentrations of ultrafine particles and their size distributions in an iron foundry using a scanning mobility particle sizer (SMPS). The 10–100 nm ultafine particle number concentrations ($NC_{0.01–0.1}$) and surface area concentrations ($SC_{0.01–0.1}$) measured at the iron foundry were 2.07×10^4 to 2.82×10^5 particles cm^{-3} and 67.56 to 2.13×10^3 µm^2 cm^{-3}, respectively. The concentrations changed dramatically depending on on-site manufacturing conditions. The $NC_{0.01–0.1}$ levels in the iron foundry were approximately 4.5 times higher on average compared with those in the outdoor ambient environment. These measurement results indicate that the presence of extra particles in the workplace air is within the ultrafine range. Additionally, the analytical results suggest that the number mode diameter can be used to estimate the $SC_{0.01–0.1}$ levels using the $NC_{0.01–0.1}$ levels. Moreover, the ultrafine particle number mode diameter was found to be about 46.1 nm in the iron foundry.
© 2008 Elsevier B.V. All rights reserved.

Keywords: Ultrafine particles; Number concentration; Surface area concentration; Scanning mobility particle sizer; Iron foundry

1. Introduction

Ultrafine particles are generally defined as particles with diameters less than 100 nm, and are largely formed through nucleation, gas-to-particle reactions or evaporation/condensation. Recent toxicological and epidemiological studies suggest that adverse pulmonary health effects are associated with freshly generated ultrafine particles [1–5]. Toxicological and epidemiological studies have also shown that ultrafine particles are more harmful from a health perspective than larger particles as smaller particles have a much larger total surface area than larger particles of the same mass, and most ultrafine particles can reach and become deposited in the alveoli region of the lung where they interact with epithelial cells [6–10]. Moreover, ultrafine particles can be transported by the blood to other

body organs such as liver within 4–24 h after exposure [3]. Transport of ultrafine particles to the brain via the olfactory nerve has recently been demonstrated [11]. Ultrafine particles concentrations are extremely threatening to environmental health.

Ultrafine particles are typically encountered in the workplace as fumes generated by combustion within saturated vapors arising from processes such as smelting, welding, soldering and plasma spraying [12]. The acute adverse effects on workers exposed to metal fumes have been well documented as metal fume fever (MFF), a self-limited, inflammatory lung disorder. Ultrafine particles play a role in mediating the adverse effects in exposed workers with MFF and other respiratory diseases [13–17]. Additionally, ultrafine particles can be generated by mechanical processes such as grinding, cutting and polishing [18].

Under normal outdoor ambient conditions, measured mean number concentrations of ultrafine particles range between 1.0×10^4 and 2.0×10^4 particles cm^{-3} [9,19–25]. Industrial processes can produce significantly higher concentrations of

ultrafine particles compared with normal outdoor ambient levels. Number concentrations of ultrafine particles in workplaces are up to >10^6 particles cm^{-3} [12,26,27]. Peak concentrations of ultrafine particles in the workplaces can be several times outdoor concentrations, and ultrafine particles generated from industrial combustion processes are important in producing adverse health effects such as respiratory diseases in susceptible individuals. However, little is known about the prevalence and magnitude of ultrafine particle concentrations in the workplace as ultrafine particles have not been as extensively monitored as other particles sizes such as PM$_{10}$, PM$_{2.5}$ or respirable levels.

Many technologies have been developed for measuring ultrafine particles *in situ* such as the condensation particle counter (CPC), scanning mobility particle sizer (SMPS), electrical low-pressure impactor (ELPI) and nanomicro-orifice cascade impactor (NanoMOUDI). These technologies measure the number, surface area or mass metric directly or indirectly [28]. Due to a lack of suitable personal samplers for ultrafine particles to assess workplace exposure and risk, measurements at fixed locations are normally adopted to determine the characteristics of worker exposure to ultrafine particles.

Ultrafine particles can be produced in iron foundry as freshly generated ultrafine particles by metal melting, pouring and molding processes. Chang et al. [29] reported that mass concentrations of PM$_{2.5}$ increased when the pouring and shakeout processes commenced in a gray iron metal casting foundry. Ultrafine particles contributed less than 1% of PM$_{2.5}$ mass, but nearly all of the particle numbers. Additionally, Evans et al. [30] measured that particle number concentrations in an automotive grey iron foundry were 7.01×10^4 to 2.76×10^5 particles cm^{-3} within the size range 10–300 nm. This study measured the number and surface area concentrations of ultrafine particles and their size distributions in an iron foundry using an SMPS to provide a more complete presentation of size-fractionated ultrafine particle characteristics via field sampling.

2. Materials and methods

2.1. Sampling site

The sampling site in this study is the casting area in an iron foundry (asterisk in Fig. 1). The iron casting operation comprises material charging, metal melting, sand mixing, molding, mold assembly, pouring, cooling, shakeout, finishing, heat treatment and inspection.

The operations performed in this sampling area are melting of raw materials, such as cast iron and steel, in a mid-frequency electric arc furnace; the heat generated by electrical power melts the solid metal into molten metal. The molten metal is then poured into a crane ladle. An overhead crane moves the crane ladle loaded with molten metal from the furnace area to the pouring area. At the pouring area, the molten metal in the crane ladle is transferred to a pouring ladle. Bottom pouring is then utilized to pour the molten metal into sand molds produced by an automatic molding machine. The casting piece is sent to the next operation area via a conveyer running through a cooling tunnel. The primary emission source of ultrafine particles in this
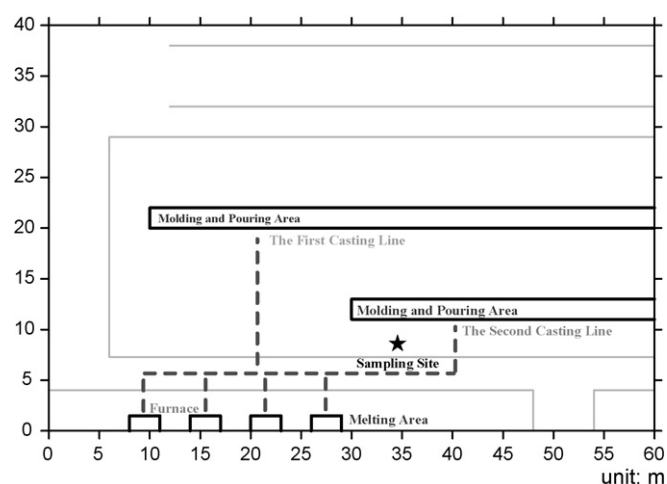

Fig. 1. Schematic diagrams of the casting area in the iron foundry. The sampling site is denoted by the asterisk, and the transport line of the crane ladle is represented by the dashed line.

operation area is generated by the operation of pouring high-temperature molten metal from the melting furnace into the crane ladle, and the subsequent operation of pouring the molten metal in crane ladle into the pouring ladle. The molten metal temperature during pouring is 1480–1520 °C.

2.2. Sampling equipment

Notably, SMPSs have been used in numerous laboratory and field studies. The SMPS system measures the number size distribution of ultrafine particles using an electrical mobility separation technique. In this study, a TSI Model 3936 Scanning Mobility Particle Sizer (TSI Inc., Shoreview, MN, USA) was utilized to measure ultrafine particles in an iron foundry. The two primary components of the TSI Model 3936 SMPS are a TSI Model 3080 Electrostatic Classifier which includes a TSI Model 3081 Differential Mobility Analyzer, and a TSI Model 3022A Condensation Particle Counter. Maximum particle concentration for the TSI Model 3022A CPC is 10^7 particles cm^{-3}. To obtain a full-size distribution of an aerosol, the SMPS is exponentially scanned by the Aerosol Instrument Manger software (AIM software).

2.3. Experimental design

The SMPS was set up in a sampling chamber to measure ultrafine particle concentrations in the workplace. A portable air conditioner was employed to keep the sampling chamber temperature <30 °C, and ensure that the CPC could be operated normally in a hot environment. The cool air generated from an air conditioner was introduced to the sampling chamber through a duct and discharged from the chamber bottom. The inlet of the sampling chamber was located at adult breathing height, roughly 1.5 m above the ground. Air was sampled through a Tygon tube roughly 0.5 m long from the sampling inlet to the SMPS. Fig. 1 shows the location of the SMPS. In this study, the SMPS was

operated at a sheath-to-sample flow ratio of 10:1. Sample flow rate in this experiment was adjusted to 1.5 L/min with a sheath air flow rate of 15 L/min to permit measuring ultrafine particles from 6 to 225 nm in diameter that were classified into 102 divisions, and to minimize diffusion losses of ultrafine particles during sampling. The SMPS data were saved at 2.25-min intervals by one scan when the SMPS up-scan time and retrace time were 120 and 15 s, respectively. The 10–100 nm ultrafine particle number concentrations ($NC_{0.01-0.1}$) and surface area concentrations ($SC_{0.01-0.1}$) were calculated from SMPS raw data. The surface area concentration was estimated from the number concentration by assuming a spherical particle geometry for the ultrafine particle. The sampling instrument was operated continuously for approximately 6–7 h during each on-site sampling period from 9 a.m. to 4 p.m. The ultrafine particle concentrations and size distributions were measured on two workdays at the iron foundry. An independent sample t-test was performed to test differences between two different sampling periods for $NC_{0.01-0.1}$ and $SC_{0.01-0.1}$ levels. A significance level of 0.05 was used for all statistical tests.

3. Results and discussion

3.1. Ultrafine particle number and surface area concentrations

Fig. 2a and b presents the time variations of $NC_{0.01-0.1}$ and $SC_{0.01-0.1}$ levels over the each sampling period. Measurement results obtained on Day 1, for $NC_{0.01-0.1}$ levels were 2.09×10^4 to 2.82×10^5 particles cm^{-3} (mean 8.33×10^4 particles cm^{-3}), and $SC_{0.01-0.1}$ levels were 2.09×10^2 to 2.13×10^3 μm^2 cm^{-3} (mean 6.32×10^2 μm^2 cm^{-3}). On Day 2, $NC_{0.01-0.1}$ levels were 2.07×10^4 to 2.82×10^5 particles cm^{-3} (mean 5.73×10^4 particles cm^{-3}) and $SC_{0.01-0.1}$ levels were 67.56 to

1.95×10^3 μm^2 cm^{-3} (mean 3.03×10^2 μm^2 cm^{-3}). Measurement results show that the great variability existed in both ultrafine particle number and surface area concentrations. Ultrafine particle number and surface area concentrations differed significantly between Days 1 and 2 ($p < 0.001$ for $NC_{0.01-0.1}$; $p < 0.001$ for $SC_{0.01-0.1}$). Measurement results indicate that the concentrations of ultrafine particles changed rapidly.

Based on the two on-site sampling results, the $NC_{0.01-0.1}$ and $SC_{0.01-0.1}$ levels measured at the iron foundry changed dramatically based on on-site manufacturing conditions. For instance, the composition of raw materials or the proportion of additives, such as nodulant and inoculant, can differ for different products and affect the ultrafine particle concentrations generated during casting operations. Variations in $NC_{0.01-0.1}$ and $SC_{0.01-0.1}$ levels during the sampling period may come from different operations. For example, fresh metal oxide fumes were emitted from the furnace and ultrafine particle levels increased when the furnace cover was opened for pouring. Based on workplace observations one could pinpoint the various activities and sources responsible for temporal variations in ultrafine particle number concentrations at a fixed location. Chang et al. [29] also pointed out that flame conditions, vaporization, thermal decomposition of organic materials, and the variability of a mold breakup during shakeout affect PM emission rates.

The $NC_{0.01-0.1}$ levels in the environment outside the factory were about 1.26×10^4 to 1.89×10^4 particles cm^{-3}, obtained by four SMPS scans during the two on-site sampling periods. Measurement results for outdoor $NC_{0.01-0.1}$ levels are similar to measurement results obtained by Tuch et al. [19], Ruuskanen et al. [22] and Pekkanen et al. [9], who measured outdoor ambient $NC_{0.01-0.1}$ levels in eastern Germany (mean $NC_{0.01-0.1} = 1.31 \times 10^4$ particles cm^{-3}), in three European cities (mean $NC_{0.01-0.1} = 1.62 \times 10^4$ to 1.83×10^4 particles cm^{-3})
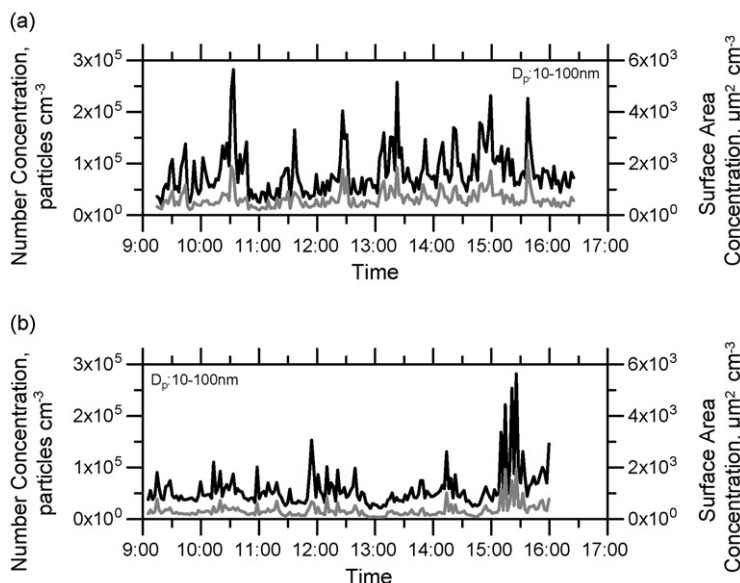

Fig. 2. Variation of $NC_{0.01-0.1}$ and $SC_{0.01-0.1}$ levels over the sampling period: (a) $NC_{0.01-0.1}$ (black line) and $SC_{0.01-0.1}$ (gray line) levels on Day 1; (b) $NC_{0.01-0.1}$ (black line) and $SC_{0.01-0.1}$ (gray line) levels on Day 2.

and in Helsinki (mean $NC_{0.01–0.1} = 1.49 \times 10^4$ particles cm^{-3}), respectively. Additionally, Rodríguez et al. [31] obtained similar results, indicating that $NC_{0.01–0.1}$ levels measured in Milan, Barcelona and London were 2.06×10^4, 1.44×10^4 and 9.33×10^3 particles cm^{-3}, respectively. In this field study, the $NC_{0.01–0.1}$ levels in an iron foundry were approximately 4.5 times higher on average compared with the outdoor ambient environment. This measurement result is similar to that obtained by Wake et al. [12], who reported that the ultrafine particle levels generated by a casting process in a zinc refinery were 2.8–4.3 times higher than those outside the refinery. These measurement results indicate that the presence of extra particles in the workplace air is within the ultrafine range. Additionally, the ultrafine particle concentrations generated from different indoor activities had been measured by Wallace [32]. The $NC_{0.01–0.1}$ levels range from 3.1×10^3 to 4.7×10^4 particles cm^{-3} for different indoor activities. The average $NC_{0.01–0.1}$ levels in an iron foundry are approximately 1.5–22.8 times higher than those indoor activities.

Fig. 3 shows the relationship between $NC_{0.01–0.1}$ and $SC_{0.01–0.1}$ derived from SMPS measurements. The linear regression relationship existing between $NC_{0.01–0.1}$ and $SC_{0.01–0.1}$ can be expressed as $Y = 7.32 \times 10^{-3}X - 31.95$ ($R^2 = 0.872$), where X is the $NC_{0.01–0.1}$ levels (in particles cm^{-3}), and Y is the $SC_{0.01–0.1}$ levels (in $\mu m^2\,cm^{-3}$). The analytical result from the slope of the linear regression indicates that the characteristic diameter of ultrafine particles (10–100 nm) is about 0.483 μm in this iron foundry. This analytical result suggests that $NC_{0.01–0.1}$ levels can be a reasonably good indicator of $SC_{0.01–0.1}$ levels with diameters the characteristic of ultrafine particles at this iron foundry. That is, the relationship between the $NC_{0.01–0.1}$ and $SC_{0.01–0.1}$ can be re-expressed as $SC_{0.01–0.1} = \pi d^2\,NC_{0.01–0.1}$, where d is 0.483 μm.
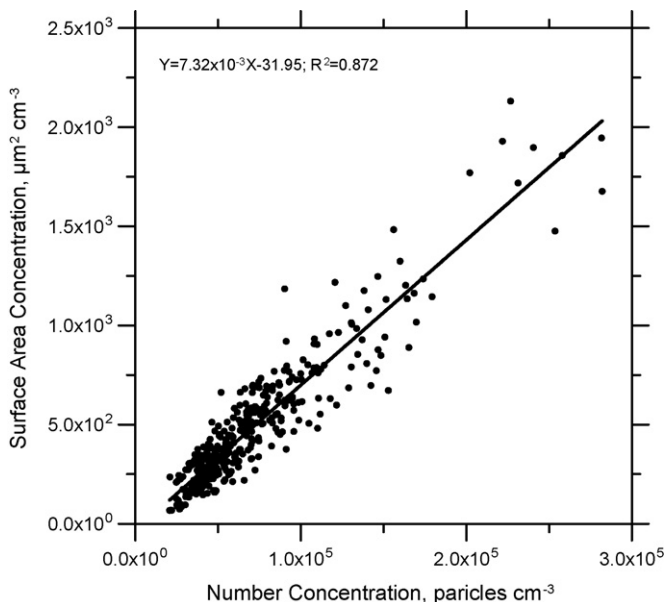

Fig. 3. The relationship between $NC_{0.01–0.1}$ and $SC_{0.01–0.1}$ based on SMPS measurements.
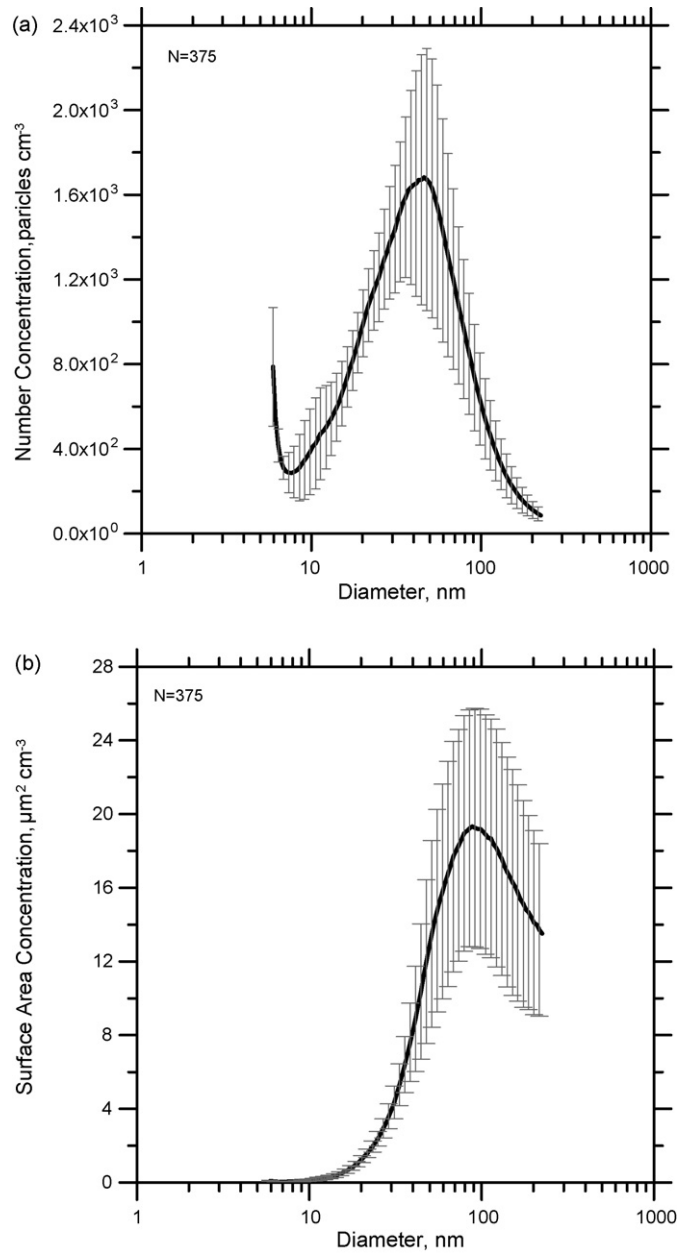

Fig. 4. Average particle number and surface area size distributions measured on two workdays by averaging data from the 375 scans by the SMPS. (a) Particle number size distribution and (b) particle surface area size distribution.

3.2. Ultrafine particle number and surface area size distribution

Fig. 4a and b shows average particle number and surface area size distributions measured on two workdays. Presented size distributions in the size range 6–225 nm were obtained by averaging data from the 375 scans by the SMPS. The upper and lower limits of the concentration error bar were defined as a single standard deviation of particle concentrations. Average particle number concentration over the two on-site sampling periods was 8.23×10^4 particles cm^{-3} within the size range 6–225 nm. Peters et al. [26] measured that particle number concentrations in an engine machining and assembly facil-

ity were 2.02×10^5 and 4.84×10^5 particles cm^{-3} in spring and winter, respectively; particles were within the size range 10–300 nm. The number concentrations inside the facility were 15–150 times greater than that those outside the facility and were highly dependent on the season. Measurement results obtained by Peters et al. for particle number concentrations in an engine machining and assembly facility were about 2.5–5.9 times higher than those measured in this study. Evans et al. [30] measured that particle number concentrations for the particle size range 10–300 nm in an automotive grey iron foundry were 1.18×10^5 particles cm^{-3} at the core-mould production area, 1.71×10^5 particles cm^{-3} at the shakeout-cleaning area and 1.60×10^6 particles cm^{-3} at the operator station near the furnace in summer. Additionally, the geometric mean number concentrations were 2.09×10^5 to 2.39×10^5 particles cm^{-3}, 1.75×10^5 to 2.76×10^5 particles cm^{-3} and 7.01×10^4 to 1.68×10^5 particles cm^{-3} in winter, spring and summer, respectively, at different areas. Measurement results obtained by Evans et al. for particle number concentrations in an automotive grey iron foundry were about 0.9–3.4 times those measured in this study.

The particle number mode, median, mean and geometric mean diameter were 46.1, 37.1, 46.2 and 35.5 nm, respectively, and the geometric standard deviation was 2.1. The particle number concentrations increased as particle diameters decreased when ultrafine particle diameters were <7 nm (Fig. 4a). The substantial amounts of ultrafine particles in this study can be attributed to fresh fumes emitted from the furnace during pouring, these particles, a few nanometers in size, were under the lower detection limit of the SMPS since the SMPS only scanned down to 6 nm. Moreover, the number median diameter of ultrafine particles measured in this study was about 0.6 times smaller than that obtained by Wake et al. [12] for a molding area at a steel foundry. Beside, the particle number mode diameter measured in this study was about 1.2–1.3 times larger than that obtained by Rodríguez et al. [31] in the urban environment in western Europe. This comparison result indicated that the particle number mode diameter in the iron foundry was larger than that in the urban environment. Additionally, the analytical characteristic diameter from slope of the linear regression (Fig. 3), 48.3 nm, is close to the number mode diameter of ultrafine particles at this iron foundry, 46.1 nm. That is, the number mode diameter of ultrafine particles and the $NC_{0.01–0.1}$ levels can be utilized to roughly estimate the $SC_{0.01–0.1}$ levels.

Additionally, average particle surface area concentration over the two on-site sampling periods was 8.59×10^2 $\mu m^2\, cm^{-3}$ for particles sized 6–225 nm. The particle surface area mode, median, mean and geometric mean diameter were 88.2, 92.0, 101.2 and 86.9 nm, respectively, and the geometric standard deviation was 1.8. Shi et al. [33] determined that the particle surface area concentrations in the ambient environment at Birmingham and Harwell were about 1.2×10^2 $\mu m^2\, cm^{-3}$ (range, 14–723 nm) and 3.0×10^2 $\mu m^2\, cm^{-3}$ (range, 11–445 nm), respectively. Moreover, ultrafine particle surface area mode diameters in the ambient environment at Birmingham and Harwell were 250 and 230 nm, respectively. Beside, Rodríguez et al. [31] obtained similar results, indicating that particle sur-

Table 1
The particle number concentrations in five selected fractions: 10–18, 18–32, 32–56, 56–100 and 100–180 nm

	Ultrafine particle size (nm)					
	10–18	18–32	32–56	56–100	100–180	10–100
Number concentration (particles cm^{-3})						
Maximum	3.20×10^4	8.88×10^4	1.29×10^5	8.22×10^5	2.71×10^4	2.82×10^5
Minimum	1.10×10^3	3.03×10^3	3.05×10^3	1.93×10^3	7.26×10^2	2.07×10^4
Mean (S.D.)	1.02×10^4 (5.46×10^3)	1.77×10^4 (1.22×10^4)	2.58×10^4 (2.05×10^4)	1.69×10^4 (1.21×10^4)	5.52×10^3 (3.48×10^3)	7.06×10^4 (4.27×10^4)
Geometric mean (GSD)	8.55×10^3 (1.90)	1.48×10^4 (1.80)	2.01×10^4 (2.02)	1.34×10^4 (1.99)	4.56×10^3 (1.89)	6.14×10^4 (1.66)

S.D.: standard deviation. G.S.D.: geometric standard deviation.

Table 2
The particle surface area concentrations in five selected fractions: 10–18, 18–32, 32–56, 56–100 and 100–180 nm

	Ultrafine particle size (nm)					
	10–18	18–32	32–56	56–100	100–180	10–100
Surface area concentration ($\mu m^2 \, cm^{-3}$)						
Maximum	20.60	1.84×10^2	7.65×10^2	1.37×10^3	1.50×10^3	2.13×10^3
Minimum	0.76	6.20	17.94	32.42	40.73	67.56
Mean (S.D.)	6.74 (3.58)	35.41 (25.37)	1.53×10^2 (1.21×10^2)	2.89×10^2 (2.05×10^2)	2.92×10^2 (1.83×10^2)	4.84×10^2 (3.35×10^2)
Geometric mean (G.S.D.)	5.73 (1.86)	29.24 (1.82)	1.19×10^2 (2.03)	2.31×10^2 (1.99)	2.43×10^2 (1.87)	3.95×10^2 (1.90)

S.D.: standard deviation. G.S.D.: geometric standard deviation.

face area mode diameters in the urban fine aerosols in Milan, Barcelona and London were 233, 179 and 198 nm, respectively. Compared with measurement results obtained by Shi et al. for particle surface area concentrations in an ambient environment were lower than those in the iron foundry by about 0.1–0.3 times and ultrafine particle surface area mode diameters in the ambient environment were larger than those in the iron foundry by about 2.6–2.8 times. These comparison results indicate that this workplace contained large number of ultrafine fume particles produced by gas-to-particle conversion. This high particle surface area concentration in the workplace can have adverse health effects. Additionally, the much lower surface area mode diameter in the foundry is caused by the much stronger formation rates of ultrafine particles than of ambient particles.

Table 1 shows the particle number concentrations in five selected fractions: 10–18, 18–32, 32–56, 56–100 and 100–180 nm for the whole measuring period of two workdays. Mean particle number concentrations for these five selected fractions were 1.02×10^4 particles cm^{-3} (13.34%), 1.77×10^4 particles cm^{-3} (23.28%), 2.58×10^4 particles cm^{-3} (33.95%), 1.69×10^4 particles cm^{-3} (22.18%) and 5.52×10^3 particles cm^{-3} (7.25%), respectively, and the mean $NC_{0.01–0.1}$ level was 7.06×10^4 particles cm^{-3}. The highest and second highest number concentrations of ultrafine particles were in fractions 32–56 and 18–32 nm, respectively, at the iron foundry. The measurement results indicated that the mean number concentrations over selected fractions were governed by particles in the size range 32–56 nm. During the two on-site sampling periods, the maximum and minimum particle number concentrations were 1.29×10^5 particles cm^{-3} (32–56 nm fraction) and 7.26×10^2 particles cm^{-3} (100–180 nm fraction), respectively.

Table 2 shows the particle surface area concentrations for the five selected fractions: 10–18, 18–32, 32–56, 56–100 and 100–180 nm. Mean particle surface area concentrations for these five selected fractions were 6.74 $\mu m^2 \, cm^{-3}$ (0.87%), 35.41 $\mu m^2 \, cm^{-3}$ (4.56%), 1.53×10^2 $\mu m^2 \, cm^{-3}$ (19.68%), 2.89×10^2 $\mu m^2 \, cm^{-3}$ (37.22%) and 2.92×10^2 $\mu m^2 \, cm^{-3}$ (37.62%), respectively, and the mean $SC_{0.01–0.1}$ level was 4.84×10^2 $\mu m^2 \, cm^{-3}$. The highest and second highest surface area concentrations of ultrafine particles were in fractions 100–180 and 56–100 nm, respectively. The measurement results suggested that the mean surface area concentrations over selected fractions were governed by particles in the size range 100–180 nm. During the two on-site sampling periods, the maximum and minimum particle surface area concentrations were 1.50×10^3 $\mu m^2 \, cm^{-3}$ (100–180 nm fraction) and 0.76 $\mu m^2 \, cm^{-3}$ (10–18 nm fraction), respectively.

4. Conclusions

The $NC_{0.01–0.1}$ and $SC_{0.01–0.1}$ levels measured at the iron foundry were 2.07×10^4 to 2.82×10^5 particles cm^{-3} and 67.56 to 2.13×10^3 $\mu m^2 \, cm^{-3}$, respectively. The concentrations changed dramatically depending on on-site manufacturing conditions. That is, ultrafine particle number and surface area concentration exposure can vary as a function of time at the iron

foundry. The $NC_{0.01-0.1}$ levels in the iron foundry were approximately 4.5 times higher on average compared with those in the outdoor ambient environment. These measurement results indicate that the presence of extra particles in the workplace within the ultrafine range. Additionally, the analytical results suggest that the number mode diameter of ultrafine particles can be used to roughly estimate $SC_{0.01-0.1}$ levels using the $NC_{0.01-0.1}$ levels. Moreover, the particle number mode diameter was found to be about 46.1 nm in the iron foundry.

Acknowledgment

References

[1] G. Oberdörster, Pulmonary effects of inhaled ultrafine particles, Int. Arch. Occup. Environ. Health 74 (2001) 1–8.

[2] K. Donaldson, D. Brown, A. Clouter, R. Duffin, W. MacNee, L. Renwick, L. Tran, V. Stone, The pulmonary toxicology of ultrafine particles, J. Aerosol Med. 15 (2002) 213–220.

[3] G. Oberdörster, Z. Sharp, V. Atudorei, A. Elder, R. Gelein, A. Lunts, W. Kreyling, C. Cox, Extrapulmonary translocation of ultrafine carbon particles following whole-body inhalation exposure of rats, J. Toxicol. Environ. Health A 65 (2002) 1531–1543.

[4] N. Englert, Fine particles and human health–a review of epidemiological studies, Toxicol. Lett. 149 (2004) 235–242.

[5] P.S. Gilmour, A. Ziesenis, E.R. Morrison, M.A. Vickers, E.M. Drost, I. Ford, E. Karg, C. Mossa, A. Schroeppel, G.A. Ferron, J. Heyder, M. Greaves, W. MacNee, K. Donaldson, Pulmonary and systemic effects of short-term inhalation exposure to ultrafine carbon black particles, Toxicol. Appl. Pharmacol. 195 (2004) 35–44.

[6] G. Oberdörster, Toxicology of ultrafine particles: in vivo studies, Philos. Trans. Roy. Soc. Lond. A 358 (2000) 2719–2740.

[7] A. Peters, H.E. Wichmann, T. Tuch, J. Heinrich, J. Heyder, Respiratory effects are associated with the number of ultrafine particles, Am. J. Respir. Crit. Care Med. 155 (1997) 1376–1383.

[8] P.A. Jaques, S.K. Chong, Measurement of total lung deposition of inhaled ultrafine particles in healthy men and women, Inhal. Toxicol. 12 (2000) 715–731.

[9] J. Pekkanen, A. Peters, G. Hoek, P. Tiittanen, B. Brunekreef, J. de Hartog, J. Heinrich, A. Ibald-Mulli, W.G. Kreyling, T. Lanki, K.L. Timonen, E. Vanninen, Particulate air pollution and risk of st-segment depression during repeated submaximal exercise tests among subjects with coronary heart disease, Circulation 106 (2002) 933–944.

[10] J.S. Brown, K.L. Zeman, W.D. Bennett, Ultrafine particle deposition and clearance in the healthy and obstructed lung, Am. J. Resp. Crit. Care Med. 166 (2002) 1240–1247.

[11] G. Oberdörster, Z. Sharp, V. Atudorei, A. Elder, R. Gelein, W. Kreyling, C. Cox, Translocation of inhaled ultrafine particles to the brain, Inhal. Toxicol. 16 (2004) 437–445.

[12] D. Wake, D. Mark, C. Northage, Ultrafine aerosols in the workplace, Ann. Occup. Hyg. 46 (S1) (2002) 235–238.

[13] H.E. Wichmann, A. Peters, Epidemiological evidence of the effects of ultrafine particle exposure, Philos. Trans. Roy. Soc. Lond. A 358 (2000) 2751–2769.

[14] W.G. Palmer, W.D. Scott, Lung cancer in ferrous foundry workers: a review, Am. Ind. Hyg. Assoc. J. 42 (1981) 329–340.

[15] P.V. Offermann, C.J. Finley, Metal fume fever, Ann. Emerg. Med. 21 (1992) 872–875.

[16] K.T. Palmer, R. McNeill-Love, J.R. Poole, D. Coggon, A.J. Frew, C.H. Linaker, J.K. Shute, Inflammatory responses to the occupational inhalation of metal fume, Eur. Respir. J. 27 (2006) 366–373.

[17] K.T. Palmer, J.R. Poole, J.G. Ayres, J. Mann, P.S. Burge, D. Coggon, Exposure to metal fume and infectious pneumonia, Am. J. Epidemiol. 157 (2003) 227–233.

[18] A.T. Zimmer, A.D. Maynard, Investigation of the aerosols produced by a high-speed, hand-held grinder using various substrates, Ann. Occup. Hyg. 46 (2002) 663–672.

[19] T. Tuch, P. Brand, H.E. Wichmann, J. Heyder, Variation of particle number and mass concentration in various size ranges of ambient aerosols in Eastern Germany, Atmos. Environ. 31 (1997) 4193–4197.

[20] L.S. Hughes, G.R. Cass, J. Gone, M. Ames, I. Olmez, Physical and chemical characterization of atmospheric ultrafine particles in the Los Angeles area, Environ. Sci. Technol. 32 (1998) 1153–1161.

[21] J.P. Shi, A.A. Khan, R.M. Harrison, Measurements of ultrafine particle concentration and size distribution in the urban atmosphere, Sci. Total Environ. 235 (1999) 51–64.

[22] J. Ruuskanen, T. Tuch, H.T. Brink, A. Peters, A. Khlystov, A. Mirme, G.P.A. Kos, B. Brunekreef, H.E. Wichmann, G. Buzorius, M. Vallius, W.G. Kreyling, J. Pekkanen, Concentrations of ultrafine, fine and $PM_{2.5}$ particles in three European cities, Atmos. Environ. 35 (2001) 3279–3738.

[23] M. Pitz, W.G. Kreyling, B. Hölscher, J. Cyrys, H.E. Wichmann, J. Heinrich, Change of the ambient particle size distribution in East Germany between 1993 and 1999, Atmos. Environ. 35 (2001) 4357–4366.

[24] S.B. Sardar, P.M. Fine, P.R. Mayo, C. Sioutas, Size-fractionated measurements of ambient ultrafine particle chemical composition in Los Angeles using the NanoMOUDI, Environ. Sci. Technol. 39 (2005) 932–944.

[25] U. Matson, Indoor and outdoor concentrations of ultrafine particles in some Scandinavian rural and urban areas, Sci. Total Environ. 343 (2005) 169–176.

[26] T.M. Peters, W.A. Heitbrink, D.E. Evans, T.J. Slavin, A.D. Maynard, The mapping of fine and ultrafine particle concentrations in an engine machining and assembly facility, Ann. Occup. Hyg. 50 (2006) 249–257.

[27] W.A. Heitbrink, D.E. Evans, T.M. Peters, T.J. Slavin, Characterization and mapping of very fine particles in an engine machining and assembly facility, J. Occup. Environ. Hyg. 4 (2007) 341–351.

[28] D.H. Brouwer, J.H.J. Gijsbers, M.W.M. Lurvink, Personal exposure to ultrafine particles in the workplace: exploring sampling techniques and strategies, Ann. Occup. Hyg. 48 (2004) 439–453.

[29] M.-C.O. Chang, J.C. Chow, J.G. Watson, C. Glowacki, S.A. Sheya, A. Prabhu, Characterization of fine particulate emissions from casting processes, Aerosol Sci. Technol. 39 (2005) 947–959.

[30] D.E. Evans, W.A. Heitbrink, T.J. Slavin, T.M. Peters, Ultrafine and respirable particles in an automotive grey iron foundry, Ann. Occup. Hyg. 52 (2008) 9–21.

[31] S. Rodríguez, R.V. Dingenen, J.P. Putaud, A. Dell'Acqua, J. Pey, X. Querol, A. Alastuey, S. Chenery, K.F. Ho, R. Harrison, R. Tardivo, B. Scarnato, V. Gemelli, A study on the relationship between mass concentrations, chemistry and number size distribution of urban fine aerosols in Milan, Barcelona and London, Atmos. Chem. Phys. 7 (2007) 2217–2232.

[32] L. Wallace, Indoor sources of ultrafine and accumulation mode particles: size distributions, size-resolved concentrations, and source strengths, Aerosol Sci. Technol. 40 (2006) 348–360.

[33] J.P. Shi, R.M. Harrison, D. Evans, Comparison of ambient particle surface area measurement by epiphaniometer and SMPS/APS, Atmos. Environ. 35 (2001) 6193–6200.